HP–HT SINTERING, MICROSTRUCTURE, AND PROPERTIES OF B_6O- AND TiC-CONTAINING COMPOSITES BASED ON cBN

D. Turkevich[1], V. Bushlya[1], I. Petrusha[2], N. Belyavina[3], V. Turkevich[1,2], J.-E. Ståhl[1]

[1]Division of Production and Materials Engineering, Lund University, Lund, Sweden
[2]Institute for Superhard Materials, NAS of Ukraine, Kiev, Ukraine
[3]Department of Physics, Shevchenko Kiev National University, Kiev, Ukraine

volodymyr.bushlya@iprod.lth.se

Abstract: Ceramic-matrix composites with a low-cBN content and different matrix compositions including B_6O and TiC have been sintered in a toroid-type high-pressure apparatus at pressure of 7.7 GPa and temperatures from 1500 to 2000°C. The microstructure, phase and elemental compositions of the produced composites have been studied using electron microscopy and XRD analysis. Mechanical properties and the performance of the sintered tool materials when turning hardened cold work tool steel have been studied.

Keywords: PCBN; boron suboxide; HP-HT sintering; cutting tools

1. INTRODUCTION

Among the cutting tool materials based on cubic boron nitride it is generally agreed to distinguish (ISO 513:2012 E) a group of materials with high-cBN content and traditionally with metal or ceramic binder produced by a reaction melting of aluminum and a group of materials having a low-cBN content and a ceramic binder (Haplin, T. *et al*., 2009). The binders in these materials with a cBN concentration of 40–60 vol% are TiC, TiN, and Ti(C,N) with an addition of a small amount of aluminum, which acts as a getter of oxygen (Angseryd, J. *et al*., 2009). It is known that in finish turning of hardened steels (Bushlya V.M. *et al.*, 2014) and heat resistant nickel superalloys (Bushlya, V. *et al*., 2013) such materials with low-cBN content exhibit higher performance than high-cBN representatives.

One of the first studies reporting the use of such binders (Hooper R.M. *et al*., 1988) states that an adhesion layer forms on the tool contact surfaces, in case of TiC modified PCBN. It is believed that it plays a protective role and inhibits a mutual diffusion of a workpiece and cutting tool elements. Nevertheless, PCBN with binders of titanium carbide and nitride have disadvantages caused by insufficiently high mechanical properties. It is known that the hardness of TiC does not exceed *HV* = 26 GPa (Ståhl J-E, 2012) and commercially produced cBN–TiC composites exhibit Knoop hardness of the order of 27 GPa. Therefore, the search for a harder or a superhard alternative to TiC and its analogues is a promising area of research. Such an alternative may be the boron suboxide, whose structure is icosahedra of boron atoms bonded by oxygen atoms (Kobayashi M. *et al*., 1993). Superhard B_6O is known for its high mechanical properties. Hardness and fracture toughness of polycrystalline boron suboxide (with addition of 2.2 vol.% Al) may attain *HV* = 32–38 GPa (Rizzo H.F. *et al.*, 1962, Sasai R. *et al.*, 2001, Itoh, H. *et al.*, 1998, Itoh, H. *et al.*, 2000) and 3 $MPa \cdot m^{1/2}$, respectively, (Shabalala T.C. *et al.*, 2008). Hardness of B_6O material decreases at a temperature of 1000°C to *HV* = 17 GPa only (Herrmann, M. *et al.*, 2011). This value is much higher than similar value for TiC (*HV* = 5 GPa) (Ståhl J-E, 2012).

The present study reports the results of a series of experiments which aimed on the sintering of the tool material based on B_6O, TiC, and cBN, which possesses a superhard binder and implements the protective mechanism of adhesion layer.

2. EXPERIMENTAL

Cubic boron nitride powder of KM grade with grain sizes of 2–3 μm (ISM, Kiev, Ukraine), B_6O powder with grain sizes of 1–2 μm, produced in FICTS (Drezden, Germany) (Shabalala T.C. *et al.*, 2008), and TiC powder with grain

sizes of 4–5 μm (H.C. STARCK, Germany) were used as the raw materials. The powder components were dry mixed by three-fold sieving through a sieve with mesh size 63x63 μm.

The experiment included sintering of three series of composites (Table 1). The series cBN–B_6O (C1) include composites with the matrix of superhard B_6O and is intended for studying the sinterability of these materials at increased pressure and temperature. The cBN–TiC series (C2) was intended to replicate the commercial materials. The series cBN–B_6O–TiC (C3) was intended to combine a superhard matrix and protective mechanism of the adhesion layer found on TiC-bound materials. The sintering was performed at a constant pressure of 7.7 GPa, sintering temperature ranged from 1500 to 2000°C. The use of higher temperature is not advisable, as contact melting may appear between boron nitride and suboxide (Solozhenko V.L. *et al.*, 2013).

Table 1. Compositions of the initial sintered mixtures and experimental conditions.

Number	Series	Compositions of the initial mixtures	Sintering temperature
1	C1	60 vol% cBN 40 vol% B_6O	1500°C 1750°C 2000°C
2	C2	60 vol% cBN 40 vol% TiC	1500°C 1750°C 2000°C
3	C3	60 vol% cBN 20 vol% B_6O 20 vol% TiC	1500°C 1750°C 2000°C

Precompacted mixtures were sintered in a toroid-type high-pressure apparatus HPAT-30 with a central hole of diameter 30 mm (Vereschagin L.F. *et al.*, 1974). The layout and the components of the assembly are given in Fig. 1. The pressure in the cell with a sample was measured via phase transformations in the Bi and PbSe standard references at room temperature. The temperature in the range of 300–2270 K was defined from the earlier established relation between the power in the electric circuit of a heater and the reading of the Pt–6% Rh/Pt–30%Rh thermocouple. Upon the stabilization of the pressure, the heating was ramped to a specified temperature for 5 s. The duration of the high-temperature sintering was 45 s followed by the released of the power and then pressure for 10 s.

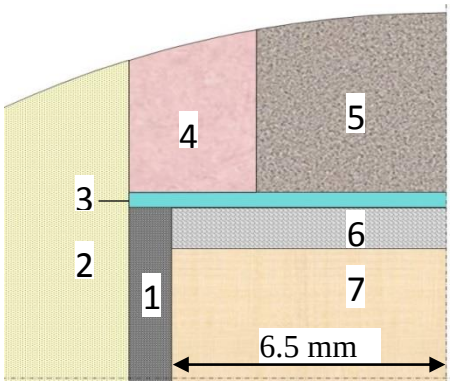

Fig. 1. Assembly of the high-pressure chamber in the HPAT-30 (a quarter of axial section): 1– heater of MG grade graphite, 2– container of lithographic stone, 3–molybdenum current lead (0.4 mm), 4– pyrophyllite heat insulation ring, 5– central heater (a mixture of graphite of the GSM grade and Zr_2O), 6–cover of GSM graphite, 7–sample.

Sintered samples were ground to RNGN090300 round inserts, according to ISO1832:2012. Prior to microscopy and indentation, the sample were polished with a diamond suspension of 9 μm and 1 μm followed by a colloidal solution of silicon oxide (0.04 μm) to produce a mirror surface. Microstructures of samples and the worn tools were studied and characterized using a Hitachi SU8010 Cold Field Emission SEM. Phase compositions of the prepared samples were defined by X-ray diffractometry in the CuK_α radiation on Mythen STOE diffractometer. Samples of the C3 series were subjected to energy dispersive X-ray spectrometry on ISIS 300 Microanalysis System. The Knoop microhardness of the composites were measured as a mean value of 5–7 indentations at a load of 4.9 N and holding time of 15 s using a Ernst Leitz Wetzlar microhardness meter.

The evaluation of the machining performance of the sintered samples was carried out when finish turning Vanadis 4E hardened cold work tool steel (58.6 HRC) (Uddeholm, 2014). The size of the wear land on the tool flank that forms when machining at a cutting speed of v_c=200 m/min, feed f = 0.15 mm/rev, and depth of cut a_c = 0.3 mm, at constant cutting length of 0.87 km, was used as the performance criterion.

3. RESULTS AND DISCUSSION

3.1. Series cBN–B_6O.

Series cBN–B_6O was planned for the study of the sinterability of composites with a low-cBN content and superhard matrix. SEM photos of the microstructure of C1–C3 series of samples were taken in secondary electrons. SEM images for EDX-mapping were taken in back scattered electrons.

It is stated in (Solozhenko V.L. *et al*., 2013) that in the in-situ experiment with powders of boron suboxide and hexagonal boron nitride neither chemical reactions and no new phase formation at temperatures up to 2430°C and pressure 5 GPa was observed, but eutectic melting of the two above phases was revealed at 2000°C. In studies of (Itoh H. *et al*., 2000) boron suboxide also did not form intermediate phases or new compounds with cBN. In current study, just like in the above studies, no reaction activity between cBN and B_6O at all sintering temperatures was observed. Figure 2 shows the results of sintering at 1750°C. The composite microstructure consists of cBN grains of size of the order of 2 μm with clear interphase boundaries between them and the surrounding matrix. The matrix is composed of large B_6O grains of sizes from 2 to 15 μm, which are formed due to the grain growth of B_6O as a result of high temperatures applied. No traces of the interaction between cBN and the matrix were revealed.

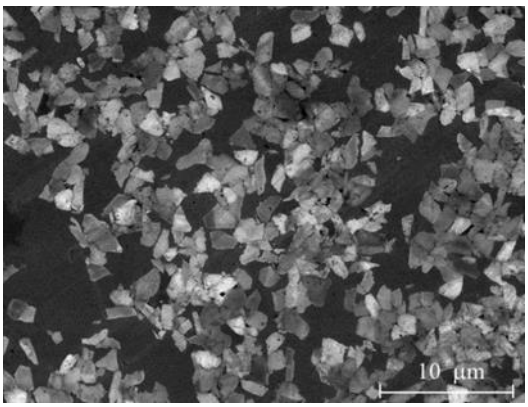

Fig. 2. SEM image of the cBN–B_6O (C1) sample sintered at 1750°C.

A diamond film of high hardness formed on the surface of a sample produced at 2000°C (Fig. 3a), which formation is in the agreement with the phenomena described in (Sozin Yu.I. *et al*., 1989, Petrusha I.A. *et al*., 2004). The diamond phase crystallizes on cBN grains. It has been suggested (Petrusha I.A. *et al*., 2004) that the structure of crystal lattice of cubic boron nitride together with p-T conditions contribute to carbon crystallization from a graphite heater in a space group $Fd\bar{3}m$. The formation of the diamond film is confirmed by the results of grazing incidence X-ray diffraction performed on the sample (Fig. 3b).

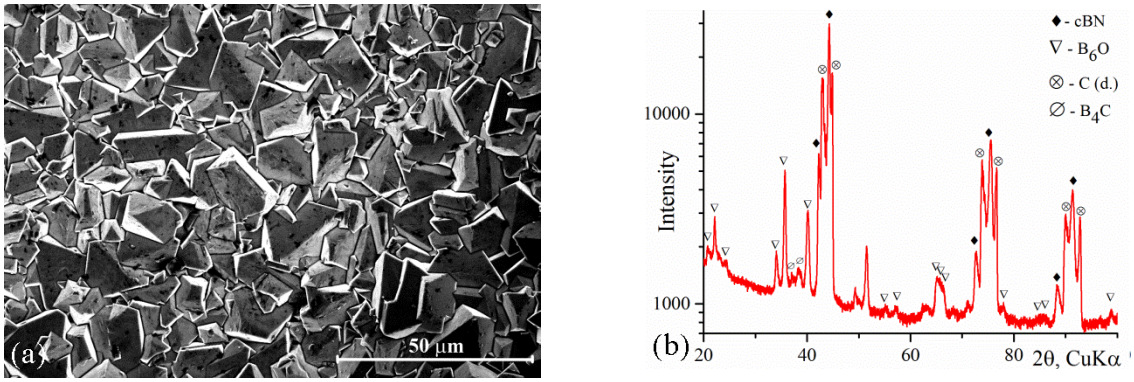

Fig. 3. SEM image of the diamond film on the cBN–B_6O (C1) sample sintered at 2000°C (a), diffraction pattern of the sample surface taken by GIS at 0.4° (b).

3.2. Series cBN–TiC.

The structure of samples of the cBN–TiC series is characterized by the presence of cBN grains of size 2–3 μm in a matrix of TiC grains of sizes from 5 to 20 μm. As in the case of samples of the C1 series, the SEM images of the sample sintered at 2000°C (Fig. 4a) do not show any traces of the interaction between the phases. However, it should be noted that the X-ray diffraction analysis given in Fig. 4b indicates the presence of minor amount of titanium diboride. It is possible that TiB_2 is generated due to the diffusion of nitrogen from cBN into TiC with the formation of the solid solution of Ti(C,N) type and a corresponding reaction of the residual boron with titanium.

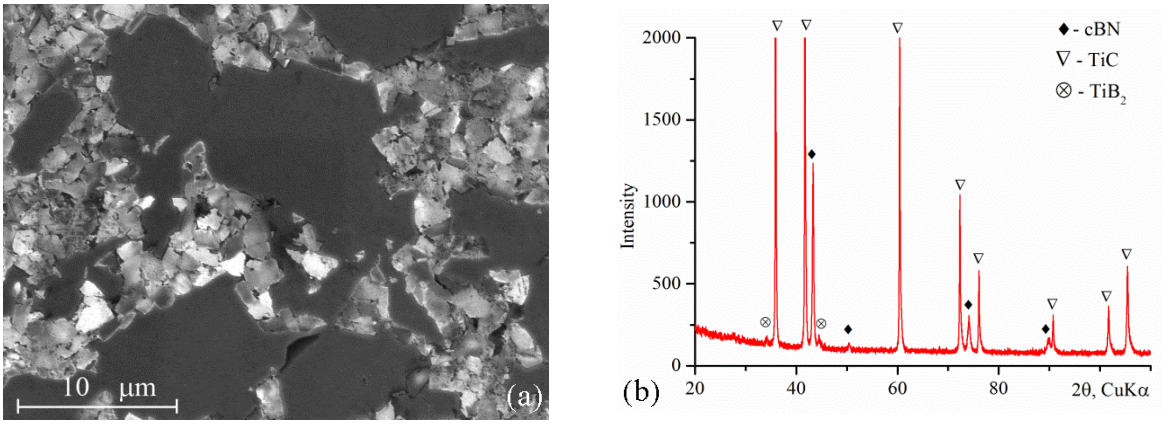

Fig. 4. SEM image (a) and diffraction pattern (b) of the cBN–TiC (C2) sample sintered at 2000°C.

3.3. Series cBN–B_6O–TiC.

Figure 5 gives a typical microstructure of a sample of the cBN–B_6O–TiC series sintered at 1500°C. As in the previous cases cBN grains have clear and unaffected grain boundaries without the signs of interaction with other phases of the composite. The matrix is composed of TiC large dark-grey grains of size up to 8 μm. Traces of the chemical interaction are visible along the edges of these grains. The products of the chemical interaction form zones approx. 0.5–2 μm thick. Also, small porous inclusions of B_6O of dark colour of size up to 3 μm are seen in the image. The existence of pores may pose the evidence of the formation of gaseous products during the HP–HT treatment.

An increase of the sintering temperature to 1750 and 2000°C leads to an increase of the amount of the reaction products caused by the intensification of the chemical interaction due to an acceleration of the mutual diffusion of reacting substances.

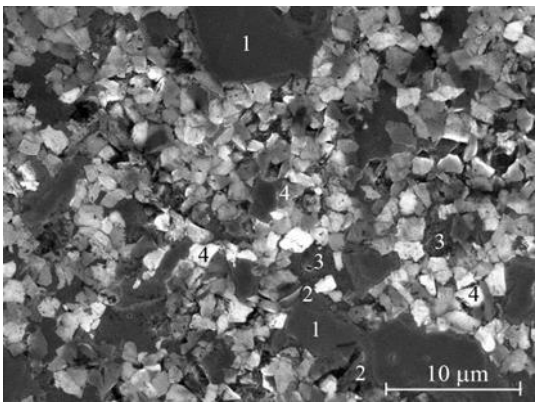

Fig. 5. SEM image of the cBN–TiC–B_6O (C3) sample sintered at 1500°C. TiC grains (1), TiB_2 fringes (2) around TiC grains, B_6O porous inclusions (3), cBN grains (4).

An EDX analysis was carried out in order to identify the products of the observed reaction. The results are given in Fig. 6.

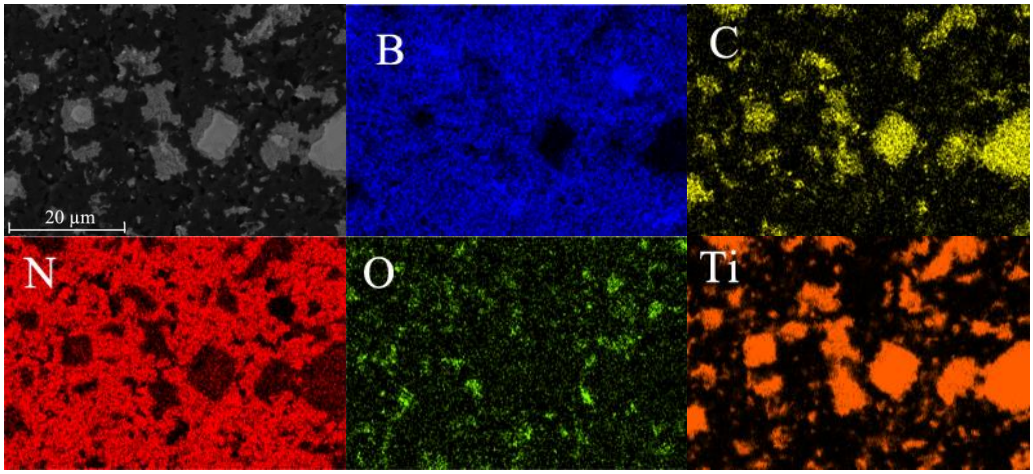

Fig. 6. EDX-mapping of the cBN–TiC–B_6O (C3) sample sintered at 2000°C.

The comparison of sample image taken in the back scattered electrons and the EDX maps indicates that dark-grey grains are comprised of boron and nitrogen and, accordingly, represent cBN. The bright regions, according to the EDX mapping, consist of titanium and carbon and grey regions, which form the fringes of the above bright regions, are composed of titanium, boron and carbon. It is believed that the grey regions are the result of a chemical interaction between B_6O and TiC which results in formation of TiB_2. Besides, as the EDX-mapping and point analysis indicate, individual grains of boron suboxide, isolated from titanium carbide by cBN grains, remained unreacted. They form porous black regions as was already mentioned in the description of the results of scanning electron microscopy. Qualitative and quantitative X-ray diffraction analyses of C3 series verifies the reaction of boron suboxide with titanium carbide and shows the appearance of lines titanium boride and boron carbide. In this case as the temperature increases, the reaction intensity increases. According to the thermodynamic calculations, the B_6O and TiC reaction at the given pressures and temperatures most likely will occur by the following equation:

$$3 \cdot B_6O + 5 \cdot TiC = 5 \cdot TiB_2 + 3 \cdot CO\uparrow + 2 \cdot B_4C \qquad (1)$$

The result of this interaction, accompanied by the formation of a gaseous phase, was observed in the analysis of the material microstructure and its phase composition. Increase of the temperature and the application pressure increase intensity of the reaction. Thus, at 1500°C the Gibbs free energy is $\Delta G_{1500} = -285$ kJ/mole and as the temperature increases to 2000°C, the Gibbs free energy becomes $\Delta G_{2000} = -465$ kJ/mole at ambient pressure. The pressure application, in turn results in the shift of the reaction equilibrium to the right: $\Delta G_{1500} = -545$ kJ/mole and $\Delta G_{2000} = -725$ kJ/mole (at 7.7 GPa), if taking the assumption that the high pressure cell is not gastight and CO leaves the reaction volume.

4. MECHANICAL PROPERTIES AND PERFORMANCE OF SAMPLES

The measured microhardness of samples of all the three series and variations of their porosity depending on the sintering temperature are given in Fig. 7.

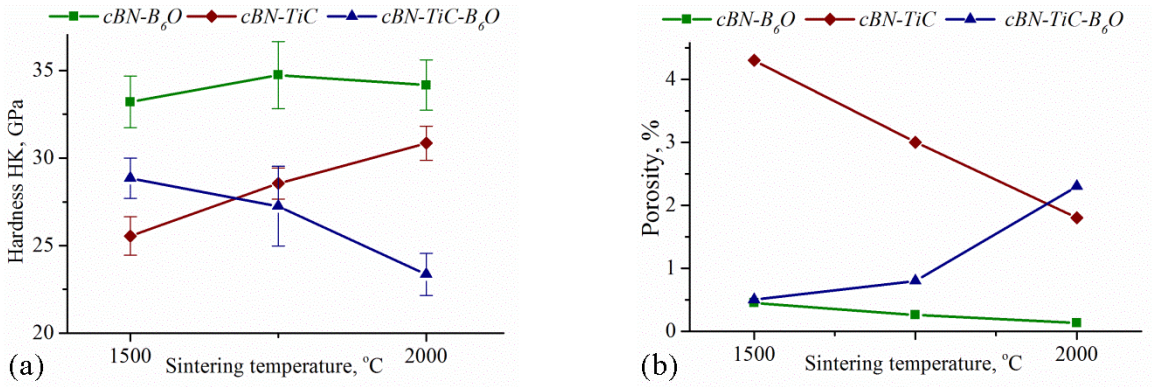

Fig. 7. Knoop microhardness of the samples (a) and porosity of the samples of C1, C2, and C3 series (b) depending on sintering temperature.

The observed variations of hardness and porosity are caused by the partial loss of oxygen by B_6O upon heating for the C1 series and the reaction between titanium carbide and boron suboxide and the formation of gaseous products according to the reaction (1) for the series C3.

The performance of the composites produced was evaluated by a number of tool wear parameters which were observed during high-speed turning Vanadis 4E hardened cold work tool steel. Typical wear morphology of tools for all sintered composites included the formation of a crater on the rake face and a wear land on the flank face (Fig. 8). A distinctive feature when machining with composites of cBN–B_6O series was the flaking on the rake face as is seen from Fig. 8a. This flaking is most likely attributed to both a low fracture toughness of composites and formation of a crater of a considerable depth and the resulting weakening of the tool microgeometry, as is shown in (Bushlya *et al*., 2013, Bushlya *et al*., 2014).

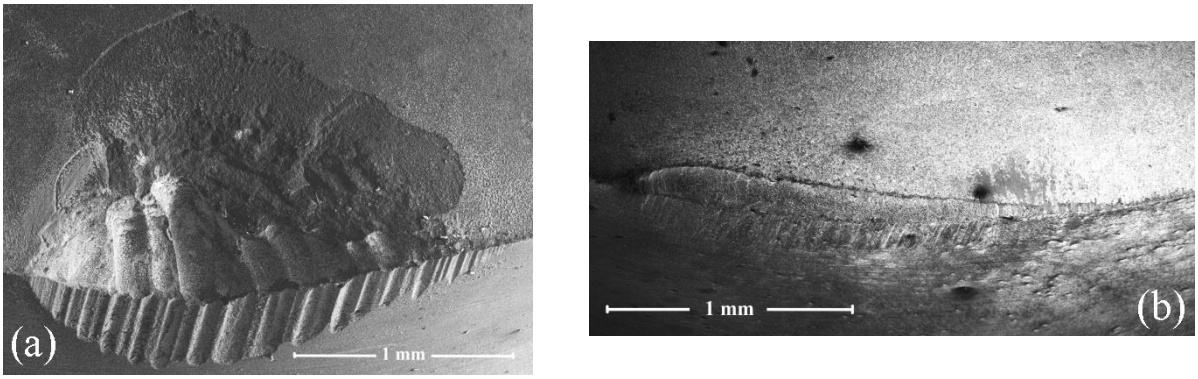

Fig. 8. Wear of (a) cBN–B_6O (C1) and (b) cBN–TiC (C2) tools sintered at 1500°C.

The poor performance of tools of the cBN–B_6O series is also evident when analyzing Fig. 9. The tool wear on the rake and flank faces exceeds similar parameters of tools of the cBN–TiC series by a factor of 5–7. For both materials, a decrease of wear with increasing sintering temperature is typical, while for the materials of cBN–B_6O–TiC series an increase of the wear takes place. This effect should be assigned to both the increase of porosity as the sintering temperature increases (Fig. 7b) and to the appearance of boron carbide forming according to reaction (1) which possesses a low strength. These effects can be evidenced by in microchipping and local fracture on tool surfaces.

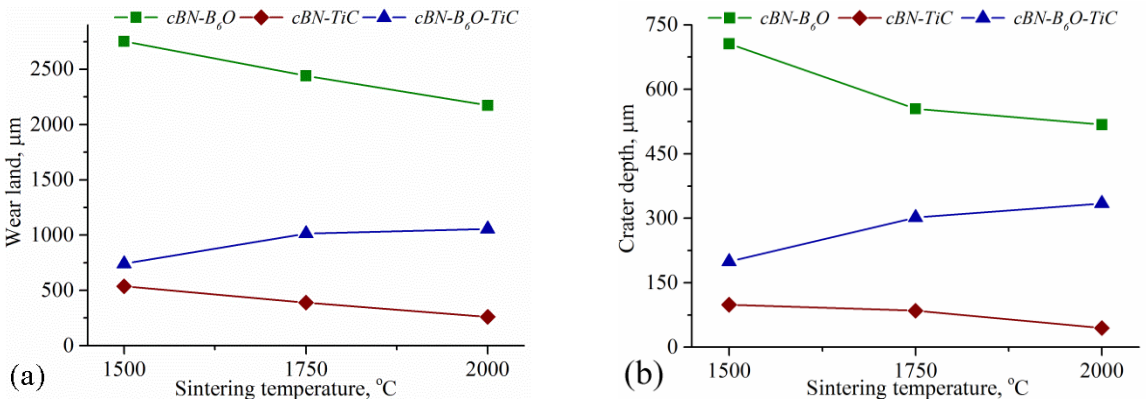

Fig. 9. Size of the flank wear land (a) and the crater depth on the rake face (b).

A closer examination of the wear surfaces at higher magnification (Fig. 10) shows that the C1 series is characterized by a predominant wear of boron suboxide, while cubic boron nitride grains remain practically untouched (Fig. 10 a).

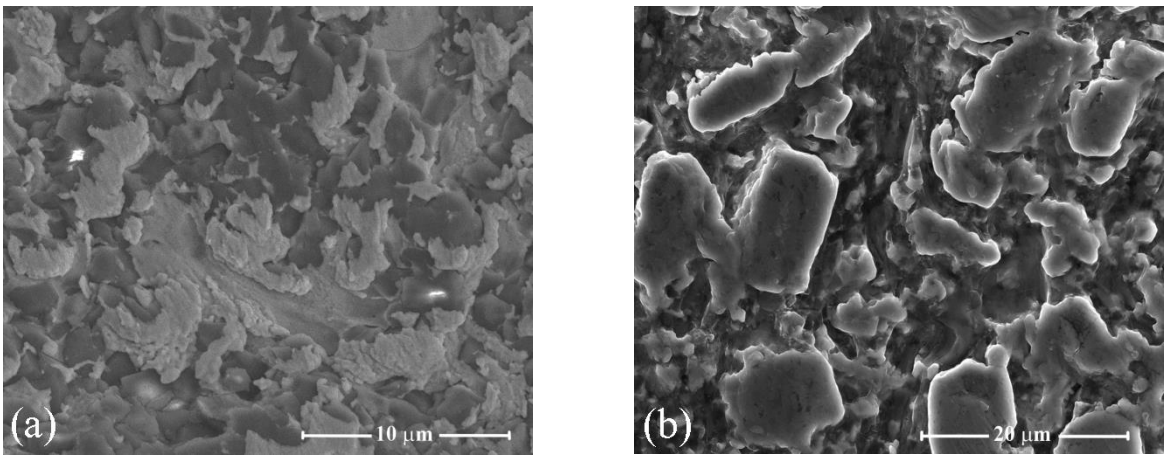

Fig. 10. SEM images of the wear surfaces of cBN–B_6O (a) and cBN–TiC (b) composites sintered at 1500°C.

Such an intensive wear of B_6O may be attributable to the material low resistance to oxidation. According to (Herrmann M. *et al*., 2011), the oxidation of boron suboxide with formation of B_2O_3 begins at 600°C, while for cBN this temperature is of the order of 1300°C. On the other hand, titanium carbide that was used as a binder in the cBN–TiC series also exhibits low resistance to oxidation, especially at temperatures above 700°C (Voitovich R.F. *et al*., 1972). However, morphology of the wear surfaces indicates a contrary wear pattern. From Fig. 10 b it is clearly seen that primarily the cubic boron nitride wears out and the large inclusions of TiC, which follow the composite microstructure (Fig. 4 a), wear to a lot lower extent. The results of the performance testing indicate that the high mechanical properties of composites of cBN–B_6O series are countered by the low chemical stability of the B_6O binder phase and in consequence these composites are essentially exceeded in performance by the composites with titanium carbide binders. The series with the B_6O and TiC binder exhibits low mechanical properties and performance, which is caused by the reaction (1) and high porosity and formation of boron carbide associated with the this reaction.

5. CONCLUSIONS.

In this study, an attempt has been made to produce composites with low-cBN content and a B_6O-based superhard matrix. Also the possibility has been considered of combining approaches including a B_6O superhard matrix with a protective adhesion layer forming in the cutting process when using TiC-bound tool materials. Three series of sintered composites have been studied. The sintering has been conducted at constant pressure of 7.7 GPa, and sintering temperatures were varied from 1500 to 2000°C. The resultant composites have been studied using scanning electron microscopy, EDX, and X-ray diffraction. Also microhardness and the performance of tools made from the composites have been assessed.

The results of the investigations indicate:

1. Composites of the cBN–B_6O series do not demonstrate any traces of reactions or formation of intermediate phases over the whole range of sintering temperatures. The composite hardness is maximum at a sintering temperature of 1750°C and attains HK=34.5 GPa.
2. Analysis of the microstructure and XRD of the composites of the cBN–TiC series does not demonstrate any reaction between the initial components as well. The hardness of the composites increases gradually with sintering temperature and attains HK=30.5 GPa.
3. When sintering composites of the cBN–TiC–B_6O series a chemical interaction between boron suboxide and titanium carbide takes place and titanium diboride and boron carbide form by the reaction $3B_6O+5TiC=5TiB_2+3CO\uparrow+2B_4C$. The intensity of the reaction significantly increases as the sintering temperature is raised. In this case, hardness of composites decreases as amount of boron suboxide in their composition decreases. It reduces from HK=29 GPa at temperature 1500°C to HK=23.5 GPa at 2000°C.
4. The highest performance of the sintered composites when turning Vanadis 4E hardened cold work tool steel was exhibited by a tool with cBN–TiC composite.

ACKNOWLEDGEMENT

This work was done as part of the Sustainable Production Initiative (SPI). The support of Uddeholm Tooling AB and S. Gunnarsson working there is greatly appreciated. The cooperation research initiative between Institute for Superhard Materials (Ukraine) and Lund University (Sweden) is also greatly acknowledged. One of the authors wishes to acknowledge a research scholarship granted by the Swedish Institute.

REFERENCES

Angseryd, J., M. Elfwing, E. Olsson, H.-O. Andrén (2009). Detailed microstructure of a cBN based cutting tool material. *International Journal of Refractory Metals and Hard Materials*, **Vol. 27 (2)**, pp. 249-255.

Bushlya, V., O. Gutnichenko, J. Zhou, P. Avdovic and J.-E. Ståhl (2013). Effects of cutting speed when turning age hardened Inconel 718 with PCBN tools of binderless and low-CBN grades. *Machining Science and Technology*, **Vol. 17 (4)**, pp. 497-523.

Bushlya, V.M., O.A. Gutnichenko, J.M. Zhou, J.-E. Ståhl and S. Gunnarsson (2014). Tool wear and tool life of PCBN, binderless cBN and wBN-cBN tools in continuous finish hard turning of cold work tool steel. *Journal of Superhard Materials*, **Vol. 36 (1)**, pp. 49-60.

Bushlya, V., J. Zhou, P. Avdovic, and J.-E. Ståhl (2013). Wear mechanisms of silicon carbide-whisker-reinforced alumina (Al2O3-SiCw) cutting tools when high-speed machining aged Alloy 718. *International Journal of Advanced Manufacturing Technology*, **Vol. 68 (5-8)**, pp. 1083-1093.

Haplin T., G. Byrne, J. Barry and Ahearne E. (2009). The Performance of Polycrystalline Cubic Boron Nitride Tools in Continuous, Semi-interrupted, and Interrupted Hard Machining. *J. Eng. Manuf.*, **Vol. 223**, pp. 947–953.

Herrmann, M., A.K. Swarnakar, M. Thiele, O. Van der Biest and I. Sigalas (2011). High temperature properties of B_6O-materials. *Journal of the European Ceramic Society*, **Vol. 31 (13)**, pp. 2387-2392.

Herrmann, M., M. Thiele, K. Jaenicke-Roessler, C.S. Freemantle, and I. Sigalas (2011). Oxidation resistance of B_6O-materials with different additives. *Journal of the European Ceramic Society*, **Vol. 31 (9)**, pp. 1771-1777.

Hooper R.M., J.I. Shakib and C.A. Brookes (1988). Microstructure and wear of TiC-Cubic BN tools. *Materials Science and Engineering - A*, **Vol. 105/106**, pp. 429–433.

ISO 513:2012 E Classification and application of hard cutting materials for metal removal with defined cutting edges - Designation of the main groups and groups of application.

Itoh, H., I. Maekawa and H. Iwahara (1998). High pressure sintering of B_6O powder and properties of sintered compact. *Journal of the Society of Materials Science*, **Vol. 47 (10)**, pp. 1000-1005.

Itoh, H., R. Yamamoto and H. Iwahara (2000). B_6O-c-BN composites prepared by high-pressure sintering. *Journal of the American Ceramic Society*, **Vol. 83 (3)**, pp. 501-506.

Kobayashi M. and I. Higashi (1993). Structure of B6O boron-suboxide by Rietveld refinement. *Journal of Materials Science*, **Vol. 28**, pp.2129-2134.

Petrusha I.A., T.I. Smirnova, A.S. Osipov and V.F. Britun (2004). Crystallization of diamond on the surface of cBN ceramics at high pressures and temperatures. *Diamond & Related Materials*, **Vol. 13**, pp. 666–670.

Rizzo H.F., W.C. Simmons and H.O. Bielstein (1962). The existence and formation of the solid B_6O. *Journal of Electrochemical Society*, **Vol. 109**, pp. 1079.

Sasai, R., H. Fukatsu, T. Kojima and H. Itoh (2001). High pressure consolidation of B_6O-diamond mixtures. *Journal of Materials Science*, **Vol. 36 (22)**, pp. 5339-5343.

Shabalala, T.C., D.S. McLachlan, I. Sigalas and M. Herrmann (2008). Hard and tough boron suboxide based composites. *Ceramics International*, **Vol. 34 (7)**, pp. 1713-1717.

Solozhenko V.L., V.Z. Turkevich, O.O. Kurakevych, D.V. Turkevich and T. Taniguchi (2013). Phase equilibria in the B-BN-B_2O_3 system at 5 GPa. *Journal of Physical Chemistry C*, **Vol. 117 (36)**, pp. 18642-18647.

Sozin Yu.I., I.A. Petrusha, and V.A. Semenovych (1989). Treatment effect of boron in nitrogen glow discharge plasma on the structural characteristics of the resulting BN. *Journal of Superhard Materials*, **Vol. 5**, pp. 11-15.

Ståhl J.-E. (2012). *Metal cutting—theories and models*. SECO Tools, Fargesta.

Vereschagin L.F., L.G. Khvorostintsev (1974). *USA Patent №3854854. High pressure apparatus*.

Voitovich R. F. and É. A. Pugach (1972). High-temperature oxidation of titanium carbide. *Soviet Powder Metallurgy and Metal Ceramics*, **Vol. 11 (2)**, pp. 132-136.

Uddeholm (2014) http://www.uddeholm.com/files/PB_Uddeholm_vanadis_4_extra_english.pdf (last accessed 12.05.2014).